Status of the Hall-D Particle Identification System

Gary Adams and Richard Heinz
1 November 2001

Introduction

One of the crucial issues in the Hall D detector design is the development of a technique to measure particle velocities, necessary for charged particle identification. This report presents the anticipated performance of the three relevant Hall D subsystems, the Cherenkov detector, the downstream time-of-flight (TOF) scintillators, and the TOF signals from the barrel calorimeter. These three systems will be used to discriminate between species of charged particles. The proposed particle identification system will discriminate between pions, kaons, and protons. Because the R&D for these subsystems is ongoing, there is of necessity some uncertainty in the results that we present. For each subsystem we discuss performance assumptions and some of the important aspects that we will be studying.

Cherenkov Subsystem

It is not possible to use TOF alone to achieve the desired level of particle discrimination unless one were to design extremely long flight paths. This conflicts with the goal of achieving large angular coverage in the spectrometer. Therefore a threshold Cherenkov detector will be used to determine the speed of high momentum tracks [1]. The radiator material was chosen to be C_4F_{10} because it offers the lowest threshold speed for an environmentally friendly gas. At atmospheric pressure this radiator has an index of refraction equal to 1.0053. This allows one to make a positive identification of pions up to about 8 GeV/c in momentum.

The current optics design is shown in Fig. 1. The detector is sectioned into sixteen identical azimuthal segments. The segments are not optically isolated. This was done to maximize the light collected for near-threshold pions. Because those tracks have a small Cherenkov angle, they will deposit all of their light in one sector, even if the track crosses a sector boundary.

Cherenkov light is piped out of the radiator volume and onto the PMT face (Burle 8854) by reflection on two mirrors. The advantage of this design is that the PMT can be moved to the downstream side of the Cherenkov box, where the fringe field is lower [2]. Also the added freedom of a second reflection allows us to place the PMT axis perpendicular to the direction of the magnetic field. This is the optimum angle for magnetic shielding. A prototype shield for the PMTs has been purchased and we expect to start testing it within a month. This shield is constructed from four cylindrical layers of high-permeability metals all on a common axis. The opening to the PMT is tapered to match the solid-angle of photons leaving the second stage mirror and entering the PMT face. The present optics require an opening angle of about ± 22 degrees. Since the first stage mirrors lie in the flight path of the TOF and LGD detectors it is necessary to minimize the amount of material that particles traverse in the mirror. These mirrors will be con-

structed from vinyl foam surrounded by carbon fiber fabric impregnated with epoxy. The mirror surface is Aluminum on Lexan with a protective coating of SiO_2.

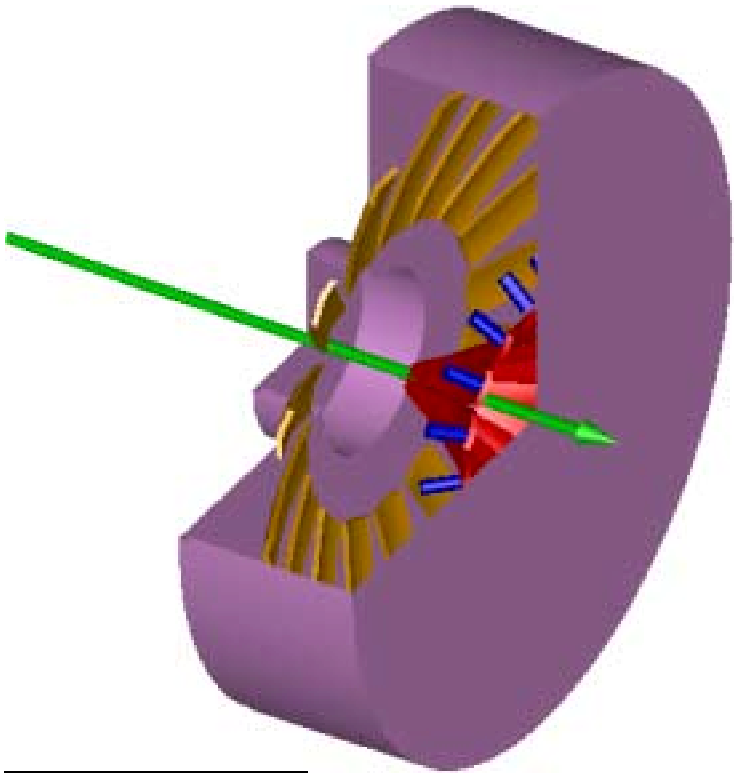

Fig. 1 - Sectioned view of the Cherenkov design.

The performance of the optics was tested with a Monte Carlo simulation. The Hall D Monte Carlo code was used to generate $K^+K^-\pi^+\pi^-$ events and transport them through the solenoid and Cherenkov detector. Photons were generated according to the velocity of the particles and randomly distributed in azimuthal angle [1]. The number of photons was attenuated by the known reflectivity of Aluminum as a function of wave length. Finally, photoelectrons were produced in the photocathode of the PMT (Burle 8854) according to the known quantum efficiency of the PMT as a function of wave length. Attenuation in the gas radiator was not included because it is negligible for high purity gas.

Fig. 2 summarizes the performance of the new optical design for tracks that hit a single first-stage mirror. The distribution of photons on the face of the PMT is shown in a scatter plot. The red points are for the central mirror sector and the blue and green points are for the PMTs in the adjacent sectors. The points at small values of X (left side of graph) are located closer to the beam axis. This figure shows that the assumed detector segmentation is nearly optimum for the

reaction of interest. Cross talk between the sectors is small for large angle pions and large for small angle pions. It also shows that a five inch pmt is adequate for this design.

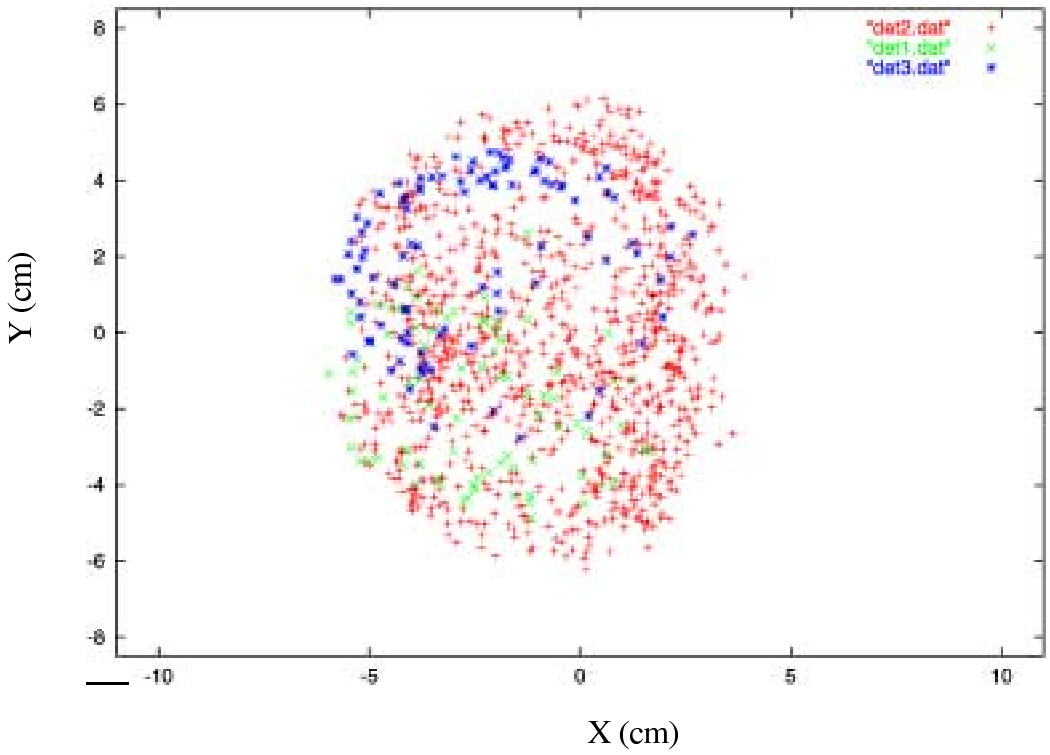

Fig. 2 - Photon distribution on the Cherenkov pmt face.

The pion detection efficiency as a function of momentum is plotted in Fig. 3 for two values of the detection threshold. The solid histogram is for a one-photoelectron threshold, and the dashed line is for a two-photoelectron threshold. These results are consistent with our earlier esti-

mates of the detection threshold [3]. They show that efficient pion identification can be made for momenta greater than about 2.9 GeV/c.

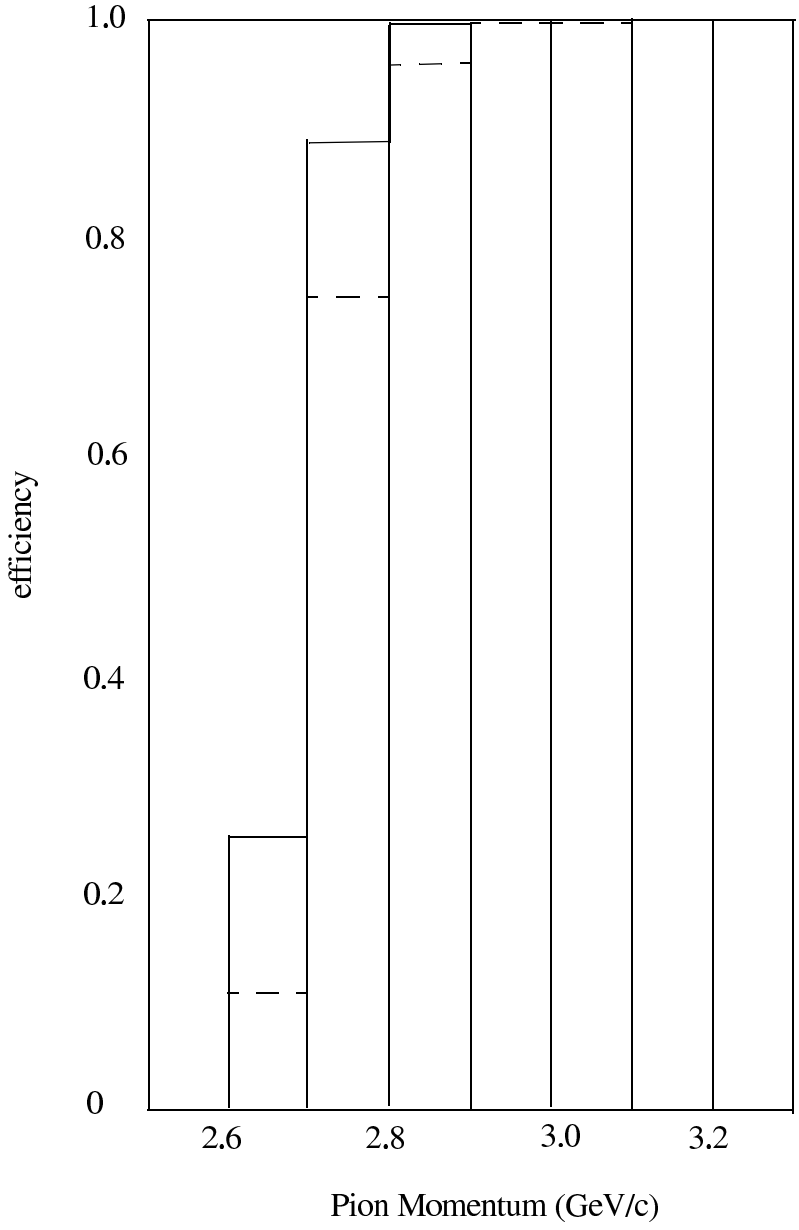

Fig. 3 - Pion detection efficiency of the Cherenkov detector.

Knock-on electrons produced by kaon interactions can result in kaons being incorectly identified as pions in the Cherenkov detector. The rate of these misidentifications will be calculated at a later time when the amount of material in front of the Cherenkov detector is better known. Based on the results of a similar detector now being used in the CLAS spectrometer one can make an order of magnitude estimate; the misidentification rate will be less than one percent of the kaon rate. Also, further simulations are needed to determine the optimum segmentation of the Cherenkov detector.

We have started to address some of the engineering issues related to the Cherenkov detector. Most of our current optical design has been incorporated into the Hall D IDEAS CAD program (Fig.1). After further refinement this design will be integrated into the Hall-D Design Report. The current detector design is more compact than the original single-mirror design. This may allow us to assemble major components of the detector off site. It is also our intention to move the design into the GEANT simulation package for Hall D.

Downstream TOF Subsystem

The TOF subsystem is composed of two walls of scintillator. Each wall is 2 m by 2 m and is formed by scintillator bars each 2 m long. The bars are horizontal in one wall, vertical in the other. At IHEP we tested bars with 2.5 cm and 5.0 cm square cross sections. We measured the time resolution as a function of the entry point of the beam particle along the 2 m dimension of the bars. Fig. 4 shows results for the two bars tested. The ordinate is the bar time resolution in picoseconds, while the abscissa indicates the entry position (along the 2.0 m bar dimension) of the beam.

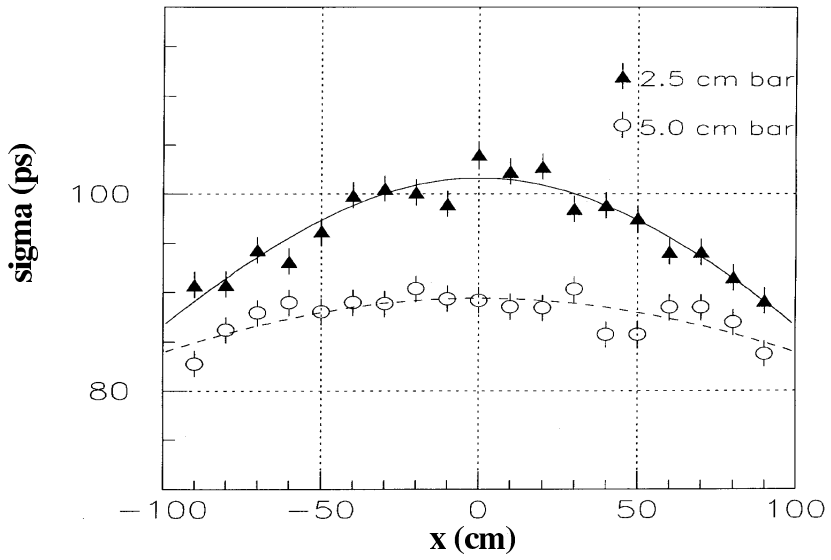

Fig. 4 - Time resolution versus entry position for the downstream TOF detectors.

Since there is a phototube (XP2020) on each end of the bar, the time resolution is worse at the center of the bar, where less total light is collected. (The effective attenuation length is about 1.4 m for the smaller bar and 2.5 m for the larger bar.) Based on these results (and granularity studies of the physics), we are planning on using 5.0 cm square bars for Hall D. The above figure shows that we will have a time resolution of 83 ps to 90 ps. The results in the above figure are an upper limit, since they do not correct for the finite size of the trigger counters, an effect of about 10%. Thus we are confident that we can achieve a resolution of 80 ps or less in the center of a 5.0 cm bar. Since there are two TOF planes, this gives an overall TOF resolution of 57 ps for the very

center of the TOF detector (if one neglects correlated errors such as the error in the common start time), better near the edges.

We are lead by the above results to state a design goal of 80 ps for the TOF subsystem. (We thus do not depend on getting signals from both planes, which would give a better resolution.) The probability of identifying a pion in the downstream TOF detector is shown in Figure 5. Here we applied the criterion that a pion is identified if its measured time-of-flight is closer to that expected from a pion than that expected from a kaon. Besides the 80 ps results (middle curve) we show the pion detection probability for 60 ps (top curve) and 100 ps (bottom curve). A comparison with Figure 3 shows how the Cerenkov and TOF subsystems complement each other. At 2.5 GeV/c, below the Cerenkov threshold for pions, the TOF is 99%, 97%, or 93% efficient at 60 ps, 80 ps, and 100 ps resolutions respectively. By 3 GeV/c the Cerenkov is essentially 100% efficient and the TOF is still over 85% efficient even for 100 ps resolution and over 90% efficient for 80 ps or better resolution.

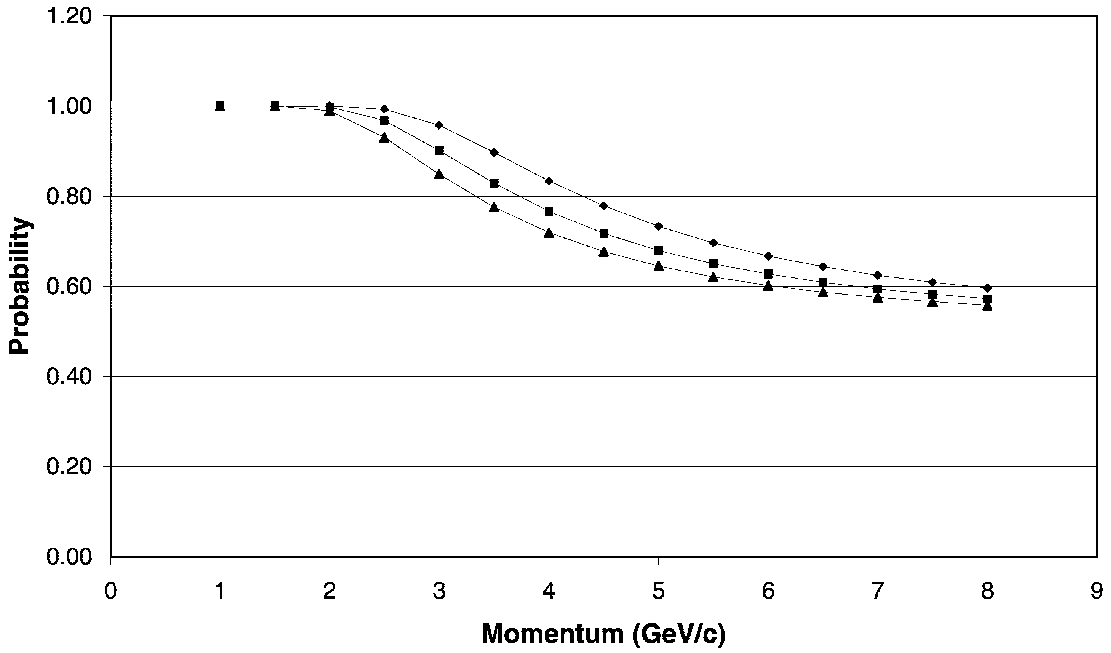

Fig. 5 - Probability of identifying a pion in the downstream TOF. The top, middle, and bottom curves are for resolutions of 60ps, 80ps, and 100ps, respectively.

There are many factors that could alter the time resolution, but these should, taken together, lead to a resolution of 80 ps or somewhat less. We list these items in categories of Diminished and Improved resolution effects.

Diminished:

1. Mass production of a subsystem consisting of many elements inevitably results in a poorer performance than that obtained in a bench test of a single element. Thus an element of the 160-element TOF walls (80 in each wall) will not achieve the resolution obtained by a single element in a test beam under ideal conditions.

2. A light pipe must be inserted between the scintillator and the PM, resulting in a loss of light.
3. We assume a perfect time resolution for the TOF common start. If the start counter can identify the RF bucket involved in the interaction, the hardware common start time can probably be corrected to less than 10 ps, which is negligible.

Improved:

1. As mentioned above there will be two scintillator walls in the TOF, and each wall will give an independent time measurement. Exceptions occur when a particle goes through a crack or through the beam hole in one of the walls.
2. At IHEP the PMTs were butted up against the scintillator, losing light relative to the final subsystem arrangement of adhesive bonding.
3. At IHEP the beam entered the scintillator normally; at Hall D the beam will in general pass through at an angle, generating more light.
4. At IHEP the 5cm by 5cm scintillator bar butted up against the 5cm diameter PM. We will see if tapering our light down to a 3.3cm circle will improve resolution by directing light onto the sweet spot of the PMT.
5. Cosmic Ray and IHEP results have shown that the TOF is sensitive to the type of constant fraction discriminator (CFD) used. We will search for a better CFD.
6. Glass may be substituted for scintillator, so that the light is prompt Cherenkov light instead of time-delayed light from fluor excitation. Also, a phototube with better time resolution could be used – an XP 2020/UR instead of an XP2020.

Barrel Calorimeter

The present design for the barrel calorimeter incorporates TOF measurements derived from timing signals measured at both ends of the Pb/Scifi bars. Based on the measured performance of similar detectors in the KLOE experiment [4] one can expect a TOF resolution of about 250 ps in our detector. While this resolution is much wider than the value expected for the downstream TOF detectors it is still a useful component of the PID system because it covers a large part of the total solid angle for charged tracks.

PID Performance

The overall performance of the PID system was estimated in a Monte Carlo simulation [2]. Useful information can also be found in earlier reports [5] that predate the final design. Ref. [2] also predates the final design but the detector parameters are very close to those described above.

In ref. [2] the HDFAST code was used to simulate the response of each of the above subsystems assuming a 9 GeV photon beam produces a single meson resonance at a mass of 2.0 GeV. The decay channel was $K^+K^-\pi^+\pi^-$. The assumed TOF resolution was 80 ps for the downstream TOF and 250 ps for the barrel calorimeter. In order to be identified by TOF the calculated difference in TOF between a pion and kaon of equal momenta was required to be less than three times the resolution of the detector at the measured momentum. This three-sigma limit will suppress pion contamination in the kaon signal by about a factor of 25.

A hard pion threshold at 2.8 GeV/c was assumed for the Cherenkov threshold. This value is slightly lower than the data in Fig. 3 would suggest. This difference is not sufficient to alter our previous conclusions.

The fraction of events that are completely determined by the PID system is only 26 percent, or about 70 percent per track. This simulation did not include any segmentation of the detectors. Therefore the low fraction of completely measured events is due to the fact that both the downstream TOF and the Cherenkov detectors span a limited angular range, and also because a rather stringent TOF requirement has been applied. However by imposing strangeness conservation one can relax the detector requirements to three resolved particles and then the event identificaton rate increases to 69 percent. Further improvements can be realized by making a kinematic fit on the remaining ambiguous tracks. The large mass difference between kaons and pions makes this a useful addition to the PID process. An overall event identification rate of 88 percent can be expected for $K^+K^-\pi^+\pi^-$ events. Although the details of the PID system remain to be worked out it is clear that the proposed combination of TOF and Cherenkov detectors will provide a good PID system for Hall D.

References

[1] See formulas 24.3 and 24.5 in The European Physical Journal C15, 2000.

[2] M. Lu and G.S. Adams, "Magnetic Simulation of the Hall D Spectrometer - Erratum," Hall D Note no. 42.

[3] M. Belis, G. Adams and J. Cummings, "PID Acceptance Using TOF, Cherenkov and Kinematic Fitting," Hall D Note no. 38.

[4] A. Antonelli, et al., Nucl. Inst. Meth. A354, 352 (1995).

[5] Curtis Meyer and Paul Eugenio, "A Study of combined K pi separation using time of flight and a gas Cherenkov detector," Hall D Note no. 15; Paul Eugenio, "A study of acceptance for the Stage 1 Hall D Detector," Hall D Note no. 16.